Imaging, Diagnosis, Prognosis

Clinical Cancer Research

Combined PET/MRI Improves Diagnostic Accuracy in Patients with Prostate Cancer: A Prospective Diagnostic Trial

Markus Hartenbach[1,5], Sabrina Hartenbach[2], Winfried Bechtloff[3], Burkhardt Danz[3], Klaus Kraft[2], Burkhard Klemenz[1], Christoph Sparwasser[4], and Marcus Hacker[5]

Abstract

Purpose: The pretherapeutic assessment of prostate cancer is challenging and still holds the risk of over- or undertreatment. This prospective trial investigates positron emission tomography (PET) with [^{18}F]fluoroethylcholine (FEC) combined with endorectal magnetic resonance imaging (MRI) for the assessment of primary prostate cancer.

Experimental design: Patients with prostate cancer based on needle biopsy findings, scheduled for radical prostatectomy, were assessed by FEC-PET and MRI in identical positioning. After prostatectomy, imaging results were compared with histologic whole-mount sections, and the PET/MRI lesion-based semiquantitative FEC uptake was compared with biopsy Gleason scores and postoperative histology.

Results: PET/MRI showed a patient-based sensitivity of 95% (36/38; 95% confidence interval (CI), 82%–99%). The analysis of 128 prostate lesions demonstrated a sensitivity/specificity/positive predictive value/negative predictive value/accuracy of 67%/35%/59%/44%/54% ($P = 0.8295$) for MRI and 85%/45%/68%/69%/68% ($P = 0.0021$) for PET, which increased to 84%/80%/85%/78%/82% ($P < 0.0001$) by combined FEC-PET/MRI in lesions >5 mm ($n = 98$). For lesions in patients with Gleason >6 tumors ($n = 43$), MRI and PET achieved 73%/31%/71%/33%/60% ($P = 1.0000$) and 90%/62%/84%/73%/81% ($P = 0.0010$), which were improved to 87%/92%/96%/75%/88% ($P < 0.0001$) by combined PET/MRI. Applying semiquantitative PET analysis, carcinomas with Gleason scores >6 were distinguished from those with Gleason $\leq$6 with a specificity of 90% and a positive predictive value of 83% ($P = 0.0011$; needle biopsy 71%/60%, $P = 0.1071$).

Conclusions: In a prospective diagnostic trial setting, combined FEC-PET/MRI achieved very high sensitivity in the detection of the dominant malignant lesion of the prostate, and markedly improved upon PET or MRI alone. Noninvasive Gleason score assessment was more precise than needle biopsy in this patient cohort. Hence, FEC-PET/MRI merits further investigation in trials of randomized, multiarm design. *Clin Cancer Res; 20(12); 3244–53. ©2014 AACR.*

Introduction

Prostate cancer is second only to nonmelanoma skin cancers as the most common cancer diagnosis affecting men in the Western world. It is, however, not the leading cause of cancer-related deaths, predominantly due to the fact that prostate cancer is a heterogeneous neoplasm concerning its aggressiveness, with peak diagnosis at the age of 69 years (1, 2). Nevertheless, the slow growing as well as the aggressive cases of this cancer (3) require tumor- and patient-adapted treatment strategies. The current guidelines offer various treatment approaches based on risk stratifications that take into account patients' prostate-specific antigen (PSA), the Gleason biopsy score and the diagnostic T stage (4), all of which suffer from certain limitations; PSA values are apt to be affected by benign and inflammatory intraprostatic changes (5), Gleason scores depend on representative needle biopsy of the main tumor focus (6), and T staging with digital rectal examination (DRE) and transrectal ultrasonography (TRUS) lacks accuracy (7, 8). These limitations imply considerable scope for improvement in the guiding of treatment.

The latest amended European guidelines recommend the use of endorectal magnetic resonance imaging (MRI) in cases in which a nonorgan-confined tumor stage is suspected and recommend the use of magnetic resonance spectroscopy (MRS), diffusion weighted images, and dynamic contrast enhanced sequences in ambiguous cases (9). Although the

Authors' Affiliations: Departments of [1]Nuclear Medicine; [2]Pathology; [3]Radiology; [4]Urology, German Armed Forces Hospital, Ulm, Germany; and [5]Division of Nuclear Medicine, Medical University of Vienna, Austria

Note: Supplementary data for this article are available at Clinical Cancer Research Online (http://clincancerres.aacrjournals.org/).

Prior presentation: Results of this work were presented at the 59th Annual Meeting of the Society of Nuclear Medicine, Miami, FL, June, 2012 (First place, Nuclear Oncology Council Young Investigator Award).

Corresponding Author: Marcus Hacker, Division of Nuclear Medicine, Medical University of Vienna, Währinger Gürtel 18–20, 1090 Vienna, Austria. Phone: 43-1-40400-5530; Fax: 43-1-40400-5532; E-mail: marcus.hacker@meduniwien.ac.at

doi: 10.1158/1078-0432.CCR-13-2653

Translational Relevance

FEC ([^{18}F]fluoroethylcholine)-PET/MRI (positron emission tomography/magnetic resonance imaging) demonstrated high sensitivity and diagnostic accuracy in the detection of clinically relevant primary prostate cancer lesions in a registered, prospective diagnostic trial design, thus presenting a reliable method for biopsy planning. In addition, the imaging results supported the fitness of a Gleason score prediction. In furthering the progress of personalized medicine, our findings could serve to reduce the number of patients subjected to over- or undertreatment. Recently developed focal therapies with significantly lower rates of therapy-related adverse effects are dependent upon a precise imaging-guided therapeutic procedure to reduce the rates of posttherapeutic tumor relapse. Furthermore, "active surveillance" strategies are still based on invasive techniques, and application of this new noninvasive diagnostic method promises to improve patient's compliance and outcome. To evaluate fully the potential of PET/MRI to assume a central position of PET/MRI in the therapeutic decision-making process, a prospective, randomized, multiarm design is mandatory for future clinical trials.

tumor detection rate of T2 weighted images is limited, especially in the central and transitional zone and results of multiparametric MRI studies are promising but heterogeneous (10–15), MRI is widely accepted as the method of choice for the assessment of tumors at the organ margins (16). Positron emission tomography (PET) with radioactive-labeled choline has shown high sensitivity with respect to prostate cancer detection (17) but with the detriment of lower specificity due to unspecific uptake in benign and inflammatory intraprostatic lesions (18). Furthermore, previous hybrid imaging studies using radiocholine PET in conjunction with CT for adding morphologic information (19, 20) suffer from limitations due to low prostate tissue contrast on CT. The significance of these studies was further compromised by the fact that PET/CT lesions were compared with histology using sextant or segmental, rather than real lesion-based analysis. Studies with whole-mount sections serving for histologic validation are hitherto only available for [^{11}C]choline (21, 22), which has slightly lower image resolution than [^{18}F]fluoroethylcholine (FEC; ref. 23), and is only available at sites with a cyclotron/radiochemistry facility due to the physical half-life of only 20 minutes for Carbon-11.

To address these shortcomings, we conducted a single-center prospective clinical trial with FEC-PET/MRI in patients with suspected prostate cancer based on positive needle biopsy who were scheduled for radical prostatovesiculectomy. We hypothesized as primary objective that the combination of FEC-PET and endorectal MRI detects and locates the largest tumor lesion in the prostate with at least 90% sensitivity and, as a secondary objective, might contribute (e.g., by semiquantitative PET analysis) to the future treatment decisions of primary localized prostate cancer. Histologically reconstructed whole-mount sections in a 100% workout of the prostate after radical prostatectomy served as the standard of reference.

Materials and Methods

The study was conducted according to Good Clinical Practice, the German pharmaceutical law (*Arzneimittelgesetz*), and radiation safety regulations (*Strahlenschutzverordnung*). We designed and carried out the study following the principles embodied in the Declaration of Helsinki and the STARD criteria for diagnostic trials. Patients' data were protected in accordance with the current German data-protection law (*Bundesdatenschutzgesetz*). Appropriate medical and liability insurance was provided for the patients. Before the study began, it had been approved by the responsible institutional ethics committee, the Federal Institute for Drugs and Medical Devices, and the Federal Office for Radiation Protection (EudraCT-No. 2006-003933-33; ClinicalTrials.gov Identifier: NCT00520546).

Included for this study were patients with histologically diagnosed prostate carcinoma based on positive needle biopsy. Patients were >50 years of age and were scheduled for radical prostatovesiculectomy the day after PET/MRI, which was conducted in a fasting condition for at least 12 hours, and at least 3 weeks following the biopsy. Exclusion criteria included all contraindications to MRI investigation, other known malignancies, surgical intervention less than 12 weeks before the PET/MRI examination, intake of choline-containing preparations, known severe liver parenchymal disorder, bronchial asthma, bradycardia, history of myocardial infarction, and intolerance of neurotropan. Most of these exclusion criteria are conditions established by the Federal Institute for Drugs and Medical Devices intended to minimize potential or hypothetical adverse effects of FEC. Data were recorded using case report forms (CRF) for each involved discipline (nuclear medicine, radiology, urology, and pathology) as well as standard operating procedures.

MRI

The MRI examination was performed using a 1.5-Tesla MRI system (Gyroscan ACS-NT; Philips) with combined QBody and endorectal coil. Pelvic assessment and lymph node staging was accomplished with 5-mm T2w turbo spin echo transverse and coronal short-tau inversion recovery sequences. For prostate assessment, 3-mm endorectal T2w spin echo sagittal, transverse, and coronal sequences were acquired. Transverse sequences were angled 90° to the intraprostatic bladder catheter to allow exact correlation with histologic whole-mount sections. A reference slice was defined in the central part of the organ, measured from the prostate base. These data guided the pathologist as a reference for the first cut of the resection preparation. Images were assessed by consensus of two

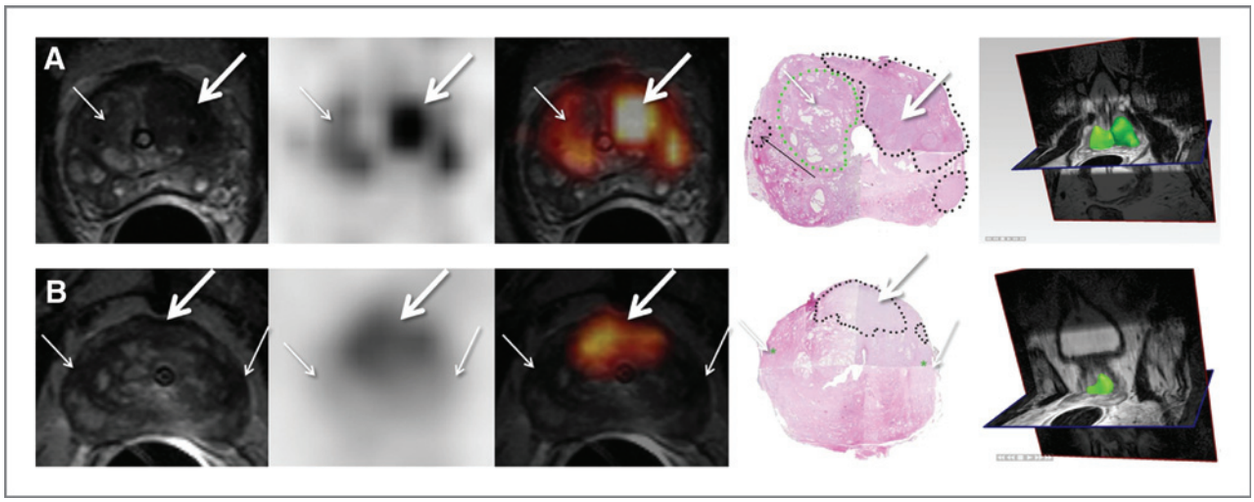

Figure 1. Endorectal T2-weighted MRI (left), FEC-PET (middle left), combined FEC-PET/MRI (middle), correlating reconstructed whole-mount section (middle right), and 3D MPR PET/MRI fusion reconstruction (right) for planning surgery (Hermes Hybrid, Hermes Medical Solutions, Stockholm, Sweden). A, improvement of PET specificity by MRI: 72-year-old man with the PSA value of 33.6 ng/mL: Both DRU and TRUS were negative. Combined PET/MRI suggested a larger tumor with Gleason score > 6 in the left transition and central zone (SUV mean t2:5.6). MRI showed localized and sharp-edged inhomogeneity, whereas PET showed a positive region signal in right central zone (light white arrow), such that combined PET/MRI suggested benign changes in that region. After surgery, a transition and central zone tumor focus on the left with Gleason score $3 + 4 = 7$ (white bold arrow) and right central benign hyperplasia (green dots) was detected. A microfocus in the right peripheral zone was not detected by PET/MRI. B, improvement of MRI specificity by PET: 69-year-old patient with PSA value of 6.6 ng/mL. MRI showed problematic assessment of the peripheral zone due to several hypointense lesions. Carcinoma was suspected, both bilaterally (light white arrows) and in the transition zone (white bold arrow). Combined PET/MRI suggested transition zone carcinoma (SUVmean, 2.8) with Gleason score $\leq$6 and no bilateral malignancy. Histology confirmed a transition zone Gleason $3 + 3 = 6$ carcinoma and postatrophic glands bilaterally being compressed by central hyperplasia (green stars), which might be the reason for T2w hyposignal.

experienced MRI radiologists (W. Bechtloff, 12 years; B. Danz, 16 years), who were blinded to the PET images and the urologic data of the patient, but aware of the study inclusion criteria. MRI-only analysis included the diagnosis of suspected tumor, T2w-hypointense intraprostatic lesions (see Supplementary Material), local staging of tumor extent, and lymph node staging of the pelvic region. Extraprostatic extension (EPE) of local tumor foci was suspected according to direct and indirect MRI signs if the prostate margins were blurred or prebulged, or if an extraprostatic hypointensity was present in the surrounding tissue. Invasion of seminal vesicles (T3b) was suspected in cases of hypointense lesions of the prostate base extending into the proximal parts or the opening of the ejaculatory duct of the seminal vesicles. Results were documented in the radiologic study Case Report Form directly after image analysis. After MRI acquisition, the modular MRI table was released from the scanner, and lifted and fixed on the PET table system. The endorectal coil was not removed until the end of the PET investigation, so as to retain tissue positions for image fusion.

PET

PET scans were performed with a lutetium oxyorthosilicate (LSO) full-ring scanner (ECAT ACCEL; Siemens) using a multiphase protocol starting with a "cold" transmission scan of the lower pelvis. This was followed by a list mode emission scan with 10 frames of one minute each, starting immediately upon administration of 3.3 MBq/kg body weight of FEC (Eckert & Ziegler EURO-PET Berlin GmbH) as a bolus through a cubital vein. After a short gap necessitated by computer processing time, the whole-body scan was performed starting at the upper thoracic aperture and proceeding down to the proximal femur. Acquisition parameters were 3 minutes per emission scan and 2 minutes per transmission scan for each of the five bed positions. As a result, the prostate region was rescanned again at $t1 = 48 (\pm 8)$ minutes after tracer injection. A delayed local acquisition of the lower pelvis at $t2 = 71 (\pm 9)$ minutes of the lower pelvis with a 6-minute emission and a 2-minute transmission scan concluded the diagnostic acquisition procedure. Image reconstruction parameters consisted of two iterations and eight subsets for whole body and delayed scans and an additional four iterations and 16 subsets in delayed local scans for sharpening focal intraprostatic FEC uptake as an aid for visual analysis. Images were reconstructed in transverse, sagittal, and coronal planes. Image assessment was obtained by consensus of two PET-experienced nuclear medicine physicians (M. Hartenbach, 11 years; B. Klemenz, 13 years) who were aware of the inclusion criteria but blinded for the MRI and histologic results. Intraprostatic focal FEC uptake exceeding the surrounding prostatic background uptake was interpreted as malignant in PET-only analysis; the semiquantitative analysis was documented as a standardized uptake value at maximum (SUV_{max}) and mean (SUV_{mean}) level (50% isoconture) using a dedicated software package (Siemens Syngo; Siemens Medical).

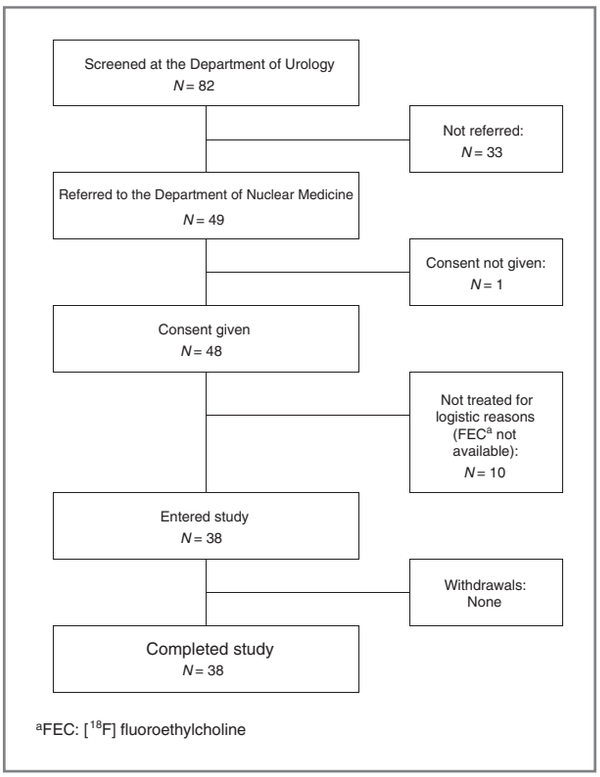

Figure 2. Patient recruitment flow diagram.

Combined PET/MRI

PET images at both time points were fused with transverse endorectal and QBody T2w MRI images using a dedicated landmark fusion tool (Multi Modality; Hermes Medical Solutions), in which the four PET/MRI fiducial markers and the arterial iliac vessels on early list mode PET images served as references. No significant registration mismatch occurred between both modalities despite the separate acquisitions. Because the assessment of PET/MRI constitutes a new approach, we initially had no strict a priori decision-making process on how to interpret the combined images. Consequently, the following algorithm was prospectively applied as a consensus of all four readers (Nuclear Medicine and Radiology; see Supplementary Material). For PET/MRI analysis, MRI-suspect lesions (as defined by the criteria above) without FEC uptake were considered nonmalignant. PET-positive and MRI-negative lesions in the central periurethral zone were also considered to be benign, for example, hyperplasia. Otherwise, MRI-suspect lesions in the central or peripheral zone in association with FEC uptake were assessed as malignant and FEC-negative areas without suspect MRI hyposignal were considered benign (see Supplementary Material). PET/MRI analysis was carried out by consensus of all four readers; PET-only analysis and PET/MRI results, including the PET-SUVmax/mean, were documented in the nuclear medicine case report form before surgery and, thus, remained blinded to the histologic results. The PET/MRI findings were prospectively printed as a hard copy for image documentation and added to the CRF facilitating, for example, the *post hoc* ROC analysis of the patient's main tumor focus as presented.

Histology

After radical prostatovesiculectomy with pelvic lymphadenectomy, the organ was fixed by immersion in formaldehyde, and rendered with different colors for each side. A reference plane from MR images was measured and taken as the first cut, as noted above. Transverse slice thickness was approximately 3 to 5 mm from apex to base. Lesions were assessed side-by-side after matching the angulation of the histologic step sections and the MRI slices. MRI-only, PET-only, and combined PET/MRI assessments were correlated with the histologically dot-marked tumor lesions. In cases of mismatch, correlating areas in histology were reassessed to classify the benign changes (see Supplementary Material).

Statistical analysis

For the primary endpoint of this open, prospective, single-arm, single-treatment, single-center study, we predicted that the patient-based sensitivity in detecting the largest intraprostatic tumor lesion by PET/MRI should exceed 90%; the relationship between the number N of observed cases and the 95% confidence interval (CI) of a probability is given by $N = 1.96^2\,P\,(1-P)/a^2$, where $P = 0.90$ (the anticipated probability) and $a = 0.095$ (the desired diagnostic accuracy for determining the probability). To achieve a lower limit of the 95% CI of at least 80%, this analysis predicts that the total of 38 patients as enrolled in the study would be sufficient (see Supplementary Material).

Data are presented in summary and/or frequency tables. Summary tables present the number of observations as well as mean, SD, minimum, median, and maximum, whereas frequency tables present absolute and relative frequencies. For determination of sensitivity, specificity, and diagnostic accuracy, "2 × 2" tables were used. These were checked for independence using the Fisher exact test at a descriptive level. The respective 95% CIs were calculated. For group statistics, in consideration that the observational units (lesions) are "clustered" within patients, the CIs were calculated for clustered samples, this being the most appropriate method for the present dataset. Analyses were made according to the formula given in McCarthy and Guo (24).

Receiver operating characteristic (ROC) analysis of SUVs and needle biopsies compared with Gleason scores was performed with the SAS PROC LOGISTIC's ROC routine (SAS Institute Inc.,). The SUV cutoff was calculated by maximizing the Youden Index and excluding any values in which sensitivity or specificity equaled 100%.

Results

Thirty-eight patients meeting study criteria were enrolled (Fig. 2). Patient and tumor characteristics are shown in Table 1. The mean (±SD) interval between biopsy and PET/MRI was 65.3 ± 6.8 days. Artefacts caused by needle biopsy potentially resulting in changes in MR T2w images or biasing assessment of the tumor extent were not detected by

Table 1. Patient characteristics

Age, y	
Mean ± SD	64.6 ± 6.5
Range	51–76
Total PSA (ng/mL; $N = 38$)	
Mean ± SD	10.5 ± 6.8
Median	8.1
Range	1.8–30.8
Days between biopsy and PET/MRI ($N = 38$)	
Mean ± SD	65.3 ± 44.4
Number of biopsies	
Mean ± SD	12.1 ± 6.1
Median	10.1
Range	6–41
Initial biopsy Gleason score[a]	
2 + 2 = 4	1 (3%)
2 + 3 = 5	3 (8%)
3 + 3 = 6	19 (50%)
3 + 4 = 7	9 (23%)
4 + 3 = 7	2 (5%)
4 + 4 = 8	3 (8%)
4 + 5 = 9	1 (3%)
5 + 4 = 9	0 (0%)
5 + 5 = 10	0 (0%)
Initial urologic risk strata[b]	
Low	6 (16%)
Intermediate	7 (18%)
High	23 (61%)
Local advanced	2 (5%)
Advanced	—
Initial urologic local staging before PET/MRI	
Organ confined	36 (95%)
Organ exceeding	2 (5%)
Histologic T stage[c] ($N = 38$)	
0	1 (3%)
2a	1 (3%)
2c	17 (45%)
3a (microfocal)	7 (18%)
3a (extensive)	5 (13%)
3b	7 (18%)
Histologic Gleason score[a] ($N = 38$)	
0	1 (3%)
2 + 2 = 4	0 (0%)
2 + 3 = 5	1 (3%)
3 + 3 = 6	20 (52%)
3 + 4 = 7	10 (26%)
4 + 3 = 7	3 (8%)
4 + 4 = 8	2 (5%)
4 + 5 = 9	0 (0%)
5 + 4 = 9	0 (0%)
5 + 5 = 10	1 (3%)
Patients with no. of lymph nodes infiltrated ($N = 38$)	
0	33 (86%)
1	3 (8%)
2	1 (3%)
3	—
4	1 (3%)
No. of lymph nodes resected per patient	
Mean ± SD	12.3 ± 4.8

[a]Gleason score ranges from 2 to 10, indicating the first and the second common type of cancer differentiation by a sum score.

[b]Urologic risk strata according to the American Urological Association (AUA) guidelines [DRE, TRUS, needle biopsy, PSA value, bone scan (PSA > 10 ng/mL)].

[c]T staging according to UICC 2002: T2a, <50% of one lobe; T2b, >50% of one lobe; T2c, both lobes; T3a, capsular invasion; T3b, invasion of seminal vesicles.

(Continued in the following column)

the pathologists. In one patient, no carcinoma was found after radical prostatectomy although his initial needle biopsy was positive. FEC-PET detected the dominant tumor focus in 36 patients (97% sensitivity; 95% CI, 86%–100%); MRI in 26 patients (70% sensitivity; 95% CI, 53%–84%); and PET/MRI in 35 patients (95% sensitivity; 95% CI, 82%–99%). The patient without histologically confirmed carcinoma was suspicious on MRI in the peripheral zone of the organ but showed no corresponding elevation of FEC uptake. PET suggested carcinoma in the central periurethral zone but in that region there was no suspicious signal detected on MRI, such that the PET/MRI analysis (see Materials and Methods) was rated as negative, as subsequently confirmed by histology.

A total of 128 intraprostatic lesions were analyzed (Table 2), including 83 foci with prostate carcinoma, 26 benign lesions positive on PET and/or PET/MRI analysis, and 19 lesions positive on MRI analysis only. By-lesion analysis showed 60% (40/67 lesions) positive prediction by MRI and 69% (59/75 lesions) by PET, and superior prediction of 87% (55/63 lesions) for the combined PET/MRI evaluation. FEC-PET and PET/MRI showed a high sensitivity of 85% (47/55) and 84% (46/55), respectively, for tumor lesions >5 mm. The combined FEC-PET/MRI evaluation significantly increased the specificity of the respective individual methods from 40% (MRI; 18/45) and 42% (PET; 19/45) to 82% (PET/MRI; 37/45) in all lesions, from 35% (MRI; 14/40) and 45% (PET; 18/40) to 80% (PET/MRI; 32/40) in patients with lesions >5 mm and from 31% (MRI; 4/13) and 62% (PET; 8/13) to 92% (PET/MRI; 12/13) in patients with Gleason score lesions exceeding 6.

The FEC-PET–positive benign lesions included 12 intraprostatic myomas, 10 areas with benign hyperplasia, three lesions (6, 8, and 13 mm) predominantly associated with

Table 2. Intraprostatic lesion analysis of endorectal MRI T2w, FEC-PET, and combined FEC-PET/eMRI in all patients, patients with malignant lesions >5 mm, and patients with Gleason score >6

	MRI	PET	PET/MRI
Lesion based all lesions ($N = 128$)			
True positive	40	59	55
False positive	27	26	8
True negative	18	19	37
False negative	43	24	28
Total true	58	78	92
Total false	70	50	36
P (Fisher exact)	0.2662	0.1699	<0.0001
PPV (%; 95% CI)	60 (58–62)	69 (67–71)	87 (85–89)
NPV (%; 95% CI)	30 (28–32)	44 (42–46)	57 (55–59)
Sensitivity (%; 95% CI)	48 (46–50)	71 (69–73)	66 (64–68)
Specificity (%; 95% CI)	40 (38–42)	42 (41–44)	82 (80–85)
Diagnostic accuracy[b] (%; 95% CI)	45 (44–47)	61 (59–63)	72 (70–74)
Lesion based without malignant lesions <5 mm ($N = 98$)			
True positive	37	47	46
False positive	26	22	8
True negative	14	18	32
False negative	18	8	9
Total true	51	65	78
Total false	44	30	17
P (Fisher exact)	0.8295	0.0021	<0.0001
PPV (%; 95% CI)	59 (57–61)	68 (66–70)	85 (83–87)
NPV (%; 95% CI)	44 (42–46)	69 (67–71)	78 (76–80)
Sensitivity (%; 95% CI)	67 (65–69)	85 (83–88)	84 (82–86)
Specificity (%; 95% CI)	35 (33–37)	45 (43–47)	80 (77–83)
Diagnostic accuracy[b] (%; 95% CI)	54 (52–55)	68 (67–70)	82 (80–84)
Lesion based in patients with Gleason >6[a] ($N = 43$)			
True positive	22	27	26
False positive	9	5	1
True negative	4	8	12
False negative	8	3	4
Total true	26	35	38
Total false	17	8	5
P (Fisher exact)	1.0000	0.0010	<0.0001
PPV (%; 95% CI)	71 (69–73)	84 (82–86)	96 (94–98)
NPV (%; 95% CI)	33 (31–35)	73 (71–75)	75 (73–77)
Sensitivity (%; 95% CI)	73 (71–76)	90 (88–92)	87 (85–89)
Specificity (%; 95% CI)	31 (29–33)	62 (60–63)	92 (90–95)
Diagnostic accuracy[b] (%; 95% CI)	60 (59–62)	81 (80–83)	88 (87–90)

[a]Gleason score ranges from 2 to 10, indicating the first and the second common type of cancer differentiation by a sum score.
[b]Diagnostic accuracy: sum of true positive + true negative among all subjects (true positive + true negative + false positive + false negative).

high-grade prostatic intraepithelial neoplasia (hgPIN) and one instance of granulocytic prostatitis. The microscopic examination of the hgPIN foci revealed no patterns for the presence of an intraductal carcinoma. MRI-positive hypointense benign lesions included formations of atrophic glands or normal prostate tissue with higher stroma density.

ROC analysis of semiquantitative SUV_{mean} t1, SUV_{mean} t2, and SUV_{max} at both time points suggested the highest area under the curve (AUC) of 0.79 for SUV_{mean} t1 in the discrimination of Gleason $\leq$6 versus Gleason >6 tumors. Table 3 presents the comparison of the ROC analysis of SUV_{mean} and Gleason scores from needle biopsy, which suggests a higher AUC (0.79 vs. 0.64) for the noninvasive semiquantitative method, although this difference did not reach significance ($P = 0.1365$). A calculated SUV_{mean} cutoff value of 3.4 presented higher specificity and

Table 3. Patient-based ROC analysis of mean standardized uptake value at 48 ± 7 minutes after injection (= t1) of FEC versus needle biopsy about Gleason >6 versus ≤6 and results of the most acceptable cutoff value 3.4 (calculated by the Youden Index)

Gleason[a] 6 vs. ≤6	SUV_{mean} t1	Needle biopsy
AUC	0.7887	0.6384
SE	0.0804	0.0816
95% CI	0.6312–0.9462	0.4785–0.7983
P	0.0029	0.1540
	SUV_{mean} t1 = 3.4	**Needle biopsy**
True positive	10	9
False positive	2	6
True negative	19	15
False negative	6	7
P (Fisher exact)	0.0011	0.1071
Sensitivity	63%	56%
Specificity	90%	71%
Diagnostic accuracy	81%	67%
PPV	83%	60%
NPV	76%	68%

[a]*N* = 37, Gleason score ranges from 2 to 10, indicating the first and the second common type of cancer differentiation by a sum score.

positive prediction of 90% (19/21 main tumor foci/patient) and 83% (10/12) as compared with the results of needle biopsy [71% (15/21) and 60% (9/15)].

Furthermore, 50% (19/38) of the study population had an organ-exceeding tumor stage (pT3a/b), including focal EPE in 7 patients and extensive EPE in 5 patients (including two cases with stage pT3b). Two of these five cases were initially detected correctly by TRUS and all of them by PET/MRI whereas none of the seven focal pT3a lesions were identified by PET/MRI. Microscopic invasion of the bladder neck or the sphincter muscles was not detected in our cohort. Five of 7 patients with seminal vesicle invasion were correctly predicted (Table 4). Five patients were found postoperatively to have positive lymph node metastases. Three patients were correctly identified as cN1 by both MRI and PET/MRI. Each of the 2 patients who were not staged correctly had one positive lymph node with metastatic occupations of 1.5 × 1- and 3.5 × 1.5-mm size (measured on histologic preparation). A *post-hoc* kappa analysis of the complete staging results, therefore, resulted in a (weighted) kappa of only 0.3871 (95% CI, 0.1423–0.6319; Table 4).

Discussion

In vivo imaging techniques currently available for clinical use show certain limitations in the detection and characterization of primary prostate cancer lesions (10–13, 19, 25, 26). Therefore, according to the current guidelines (9), the standardized diagnostic procedure for patients with suspected prostate cancer, is still based upon the serum PSA value, the DRE and TRUS, ultimately leading to sampling of the organ by a standardized needle biopsy (27). Together, the biopsy Gleason score, PSA level, and the clinical tumor stage then enable a rational risk stratification and treatment decision, which is mainly based upon nomograms providing a range of probabilities for each tumor stage. Although invasive techniques are used for these statistically based predictions, the predictive accuracy has not surpassed 70% to 80% (28). Although PSA values may also be increased in the presence of benign prostate hyperplasia or infections (5), the Gleason score can be a more robust surrogate marker for tumor aggressiveness, when it is determined from representative biopsies of the main prostate cancer focus. In practice, these areas are frequently missed, however, and studies have found only a weak concordance between biopsy findings and postoperative Gleason scores of 54% (29), underscoring the need for a noninvasive diagnostic method with a high tumor detection rate, and improved tumor characterization.

The present prospective diagnostic trial demonstrated high patient-based sensitivity for FEC-PET and combined

Table 4. Local staging results of FEC-PET/MRI compared with the histologic results *N* = 38

	Histologically ascertained T stage[a]					
	0	**2a**	**2c**	**3a**	**3b**	**Total**
T stage found by PET/MRI						
0	1	—	—	—	—	1
2a		—	—	2	—	2
2c	—	2	9	5	—	16
3a	—	—	5	3	2	10
3b	—	—	2	2	5	9
Total	1	2	16	12	7	38

[a]T staging according to UICC 2002: T2a, < 50% of one lobe; T2b, > 50% of one lobe; T2c, both lobes; T3a, capsular invasion; T3b, invasion of seminal vesicles.

FEC-PET/MRI in the detection of the dominant prostate cancer lesion in a cohort of 38 patients who underwent resective surgery after positive biopsy. This encouraging finding is mainly derived from the high sensitivity of the FEC-PET metabolic method. The morphologic imaging with MRI T2w in this study showed results, which are in line with recently published data (12, 15). Nevertheless, it is clear that some degree of false-positive or -negative findings is to be expected from the MRI-only analysis, insofar as the two radiologists had to come to a concordant decision (benign/malignant) even in ambiguous or indeterminate lesions. A further limitation of our analysis may arise from the positive work-up bias of this first prospective FEC-PET/MRI study, in that all the mean were known to have had positive needle biopsies. This bias was limited as far as in that the patient-based analysis had to detect in each patient the largest malignant lesion exactly matching the histologic whole-mount section.

It should be noted that the use of multiparametric MRI techniques up to 3-Tesla is indeed superior to T2w images for detecting lesions in the peripheral zone of the prostate, as reported in literature (12, 15). Nonetheless, even such high field MRI did not attain the diagnostic accuracy of our presented data of combined FEC-PET/MRI. Therefore, our multimodal imaging method emerges as especially helpful in transition zone prostate cancer in which other techniques are still of limited value (12). Even though addition of MRS was not possible in our study due to the intraprostatic bladder catheter, our findings supports the initial aspiration of our trial, which was to improve the metabolic imaging with FEC-PET, by adding only morphologic information from MRI; this significantly reduced patients' total scanning time. Applying lesion based analysis, both PPV and specificity of both single modalities markedly increased with the hybrid technique, yielding to a significant reduction in false positive findings, which may plausibly support more precise image guided biopsies in the future.

The results of combined FEC-PET/MRI were notably superior in tumor lesions >5 mm. Here, the added sensitivity of the combined imaging was dominated by the PET instrumentation, as the resolution of the PET scanner used in the present trial was limited to about 6 mm. We anticipate that recently introduced PET/MRI hybrid scanners shall provide still more accurate findings in tumor sizes below 5 mm (30, 31). There are, in any case, strong correlations between tumor size and both pathologic stage and tumor aggressiveness based on the Gleason score (32), which calls into question the clinical relevance of tumors below 5 mm. Furthermore, the detection of the leading intraprostatic tumor lesion is most important for the successful execution of needle biopsies, especially in patients with persisting PSA elevations and inconspicuous first biopsy.

A secondary objective of our study was to assess tumor characteristics by the combined imaging, as a potential factor in improved therapeutic regimens in patients with prostate cancer. Placing our particular focus on the more aggressive tumor subtypes with Gleason scores >6, the addition of FEC-PET data enhanced the sensitivity of MRI alone from 73% to 87% and the specificity from 31% to 92%. In addition, findings of elevated FEC-PET standardized uptake values in individual lesions (SUV_{mean} t1) were significantly ($P = 0.0011$) associated with tumors of higher Gleason scores (>6) at by-lesion analysis, whereas the results of the needle biopsy did not reach statistical significance in this cohort ($P = 0.1071$). No hitherto published prospective study of FEC-PET has suggested an association between PET parameters and the Gleason score. Initial [^{11}C]-choline-PET/CT studies with acquisition times starting from 5 to 10 minutes after injection, reported no such significant correlation (33, 34). But supporting the present findings, a recently published study using [^{11}C]-choline PET/CT and MRI, did indicate a correlation between choline uptake combined with MRI diffusion coefficient maps and Gleason scores in 17 patients (21).

The manifest ability of FEC-PET/MRI to discriminate between the more aggressive cancers with Gleason scores >6 and the potentially slower-growing tumor types in the present patient cohort might suggest the feasibility of new urologic diagnostic strategies, including "watchful waiting" and "active surveillance" based on semiquantitative FEC-PET/MRI analyses. This is also supported by our finding that combined PET/MRI staging detected seminal vesicle invasion in five of seven and excessive EPE in 5 of 5 patients, both of these observations are important parameters for individualized management when considering external radiotherapy or nerve sparing radical prostatectomy. These promising results have to be evaluated in a larger cohort of high-risk patients.

A recent clinical study did not report any significant differences between the mortality of patients with clinically localized prostate cancer and a PSA value of <50 ng/mL treated with "radical prostatectomy" versus "observation only" during a 10 years follow-up. However, radical prostatectomy was possibly associated with a decrease in all-cause mortality in intermediate- and high-risk tumors (35). Furthermore, recently developed focal therapies with significantly lower rates of therapy-related adverse effects have come to depend on high spatial precision of imaging-guided therapy so as to reduce optimally the rates of post-therapeutic tumor relapse (36). Taking these facts into account and in support for the strategy of personalized medicine, the high sensitivity of noninvasive FEC-PET/MRI combined with the capacity for a precise lesion classification promises to reduce the number of patients subjected to over- or undertreatment and should also enhance the success rate of needle biopsies targeting the clinically significant tumor lesion.

Disclosure of Potential Conflicts of Interest

No potential conflicts of interest were disclosed.

Authors' Contributions

Conception and design: M. Hartenbach, S. Hartenbach, W. Bechtloff, C. Sparwasser

Development of methodology: M. Hartenbach, S. Hartenbach, C. Sparwasser

Acquisition of data (provided animals, acquired and managed patients, provided facilities, etc.): M. Hartenbach, S. Hartenbach, W. Bechtloff, B. Danz, B. Klemenz, C. Sparwasser
Analysis and interpretation of data (e.g., statistical analysis, biostatistics, computational analysis): M. Hartenbach, K. Kraft, B. Klemenz, C. Sparwasser, M. Hacker
Writing, review, and/or revision of the manuscript: M. Hartenbach, S. Hartenbach, B. Klemenz, C. Sparwasser, M. Hacker
Administrative, technical, or material support (i.e., reporting or organizing data, constructing databases): M. Hartenbach, S. Hartenbach, W. Bechtloff, B. Klemenz, C. Sparwasser, M. Hacker
Study supervision: M. Hartenbach, S. Hartenbach, B. Klemenz, C. Sparwasser

Acknowledgments

The authors thank Andrea Schuessele, Ph.D. (Eckert & Ziegler Radiopharma GmbH, Berlin, Germany) and Peter Jaehnig (pj-Statistics, Berlin, Germany) for assistance with the data and statistical analysis and the final ICH-compliant study report; and to the personnel of the Departments of Urology, Pathology, Radiology and Nuclear Medicine at the Federal Armed Forces Hospital, Ulm, Germany, for executing the investigations. Medical writing assistance and revision of the article was provided by Richard A. Mason, M.D. (Case Western Reserve University School of Medicine, Cleveland, OH), and the authors thank the additional editing expertise of Inglewood Biomedical Editing.

The investigational pharmaceutical product FEC was supplied by Eckert & Ziegler EUROPET Berlin GmbH, Berlin, Germany, and regulated in a separate contract with the Federal Armed Forces Hospital, Ulm, Germany. This contract comprised the use of study outcome data for achieving the marketing authorization of FEC-Max, solution for injection, by the German Federal Institute for Drugs and Medical Devices.

Grant Support

This study was supported by the German Federal Ministry of Defense special research fund (grant number 12K3-S-140708).

The costs of publication of this article were defrayed in part by the payment of page charges. This article must therefore be hereby marked *advertisement* in accordance with 18 U.S.C. Section 1734 solely to indicate this fact.

Received September 26, 2013; revised March 3, 2014; accepted March 25, 2014; published OnlineFirst April 24, 2014.

References

1. Haberland J, Bertz J, Wolf U, Ziese T, Kurth BM. German cancer statistics 2004. BMC cancer 2010;10:52.
2. Siegel R, Naishadham D, Jemal A. Cancer statistics, 2012. CA Cancer J Clin 2012;62:10–29.
3. Mouraviev V, Villers A, Bostwick DG, Wheeler TM, Montironi R, Polascik TJ. Understanding the pathological features of focality, grade and tumour volume of early-stage prostate cancer as a foundation for parenchyma-sparing prostate cancer therapies: active surveillance and focal targeted therapy. BJU Int 2011;108:1074–85.
4. Thompson I, Thrasher JB, Aus G, Burnett AL, Canby-Hagino ED, Cookson MS, et al. Guideline for the management of clinically localized prostate cancer: 2007 update. J Urol 2007;177:2106–31.
5. Greene KL, Albertsen PC, Babaian RJ, Carter HB, Gann PH, Han M, et al. Prostate-specific antigen best practice statement: 2009 update. J Urol 2009;182:2232–41.
6. King CR, Patel DA, Terris MK. Prostate biopsy volume indices do not predict for significant Gleason upgrading. Am J Clin Oncol 2005; 28:125–9.
7. Halpern EJ, Strup SE. Using gray-scale and color and power Doppler sonography to detect prostatic cancer. AJR Am J Roentgenol 2000; 174:623–7.
8. Mistry K, Cable G. Meta-analysis of prostate-specific antigen and digital rectal examination as screening tests for prostate carcinoma. J Am Board Fam Pract 2003;16:95–101.
9. Heidenreich A, Bellmunt J, Bolla M, Joniau S, Mason M, Matveev V, et al. EAU guidelines on prostate cancer. Part 1: screening, diagnosis, and treatment of clinically localised disease. Eur Urol 2011;59:61–71.
10. Amsellem-Ouazana D, Younes P, Conquy S, Peyromaure M, Flam T, Debre B, et al. Negative prostatic biopsies in patients with a high risk of prostate cancer. Is the combination of endorectal MRI and magnetic resonance spectroscopy imaging (MRSI) a useful tool? A preliminary study. Eur Urol 2005;47:582–6.
11. Hara N, Okuizumi M, Koike H, Kawaguchi M, Bilim V. Dynamic contrast-enhanced magnetic resonance imaging (DCE-MRI) is a useful modality for the precise detection and staging of early prostate cancer. Prostate 2005;62:140–7.
12. Hoeks CM, Hambrock T, Yakar D, Hulsbergen-van de Kaa CA, Feuth T, Witjes JA, et al. Transition zone prostate cancer: detection and localization with 3-T multiparametric MR imaging. Radiology 2013;266: 207–17.
13. Li H, Sugimura K, Kaji Y, Kitamura Y, Fujii M, Hara I, et al. Conventional MRI capabilities in the diagnosis of prostate cancer in the transition zone. AJR Am J Roentgenol 2006;186:729–42.
14. Ocak I, Bernardo M, Metzger G, Barrett T, Pinto P, Albert PS, et al. Dynamic contrast-enhanced MRI of prostate cancer at 3 T: a study of pharmacokinetic parameters. AJR Am J Roentgenol 2007;189:849.
15. Wu LM, Xu JR, Ye YQ, Lu Q, Hu JN. The clinical value of diffusion-weighted imaging in combination with T2-weighted imaging in diagnosing prostate carcinoma: a systematic review and meta-analysis. AJR Am J Roentgenol 2012;199:103–10.
16. Engelbrecht MR, Jager GJ, Laheij RJ, Verbeek AL, van Lier HJ, Barentsz JO. Local staging of prostate cancer using magnetic resonance imaging: a meta-analysis. Eur Radiol 2002;12:2294–302.
17. Umbehr MH, Muntener M, Hany T, Sulser T, Bachmann LM. The role of 11C-choline and 18F-fluorocholine positron emission tomography (PET) and PET/CT in prostate cancer: a systematic review and meta-analysis. Eur Urol 2013;64:106–17.
18. Li X, Liu Q, Wang M, Jin X, Yao S, Liu S, et al. C-11 choline PET/CT imaging for differentiating malignant from benign prostate lesions. Clin Nucl Med 2008;33:671–6.
19. Beheshti M, Imamovic L, Broinger G, Vali R, Waldenberger P, Stoiber F, et al. 18F choline PET/CT in the preoperative staging of prostate cancer in patients with intermediate or high risk of extracapsular disease: a prospective study of 130 patients. Radiology 2010;254:925–33.
20. Giovacchini G, Picchio M, Coradeschi E, Scattoni V, Bettinardi V, Cozzarini C, et al. [(11)C]choline uptake with PET/CT for the initial diagnosis of prostate cancer: relation to PSA levels, tumour stage and anti-androgenic therapy. Eur J Nucl Med Mol imaging 2008;35: 1065–73.
21. Park H, Wood D, Hussain H, Meyer CR, Shah RB, Johnson TD, et al. Introducing parametric fusion PET/MRI of primary prostate cancer. J Nucl Med 2012;53:546–51.
22. Souvatzoglou M, Weirich G, Schwarzenboeck S, Maurer T, Schuster T, Bundschuh RA, et al. The sensitivity of [11C]choline PET/CT to localize prostate cancer depends on the tumor configuration. Clin Cancer Res 2011;17:3751–9.
23. Hara T, Kosaka N, Kishi H. Development of (18)F-fluoroethylcholine for cancer imaging with PET: synthesis, biochemistry, and prostate cancer imaging. J Nucl Med 2002;43:187–99.
24. McCarthy WF, Guo N. The estimation of sensitivity and specificity of clustered binary data. Proc SUGI 2006;31:206–31.
25. Haider MA, van der Kwast TH, Tanguay J, Evans AJ, Hashmi AT, Lockwood G, et al. Combined T2-weighted and diffusion-weighted MRI for localization of prostate cancer. AJR Am J Roentgenol 2007;189:323–8.
26. Yuen JS, Thng CH, Tan PH, Khin LW, Phee SJ, Xiao D, et al. Endorectal magnetic resonance imaging and spectroscopy for the detection of tumor foci in men with prior negative transrectal ultrasound prostate biopsy. J Urol 2004;171:1482–6.
27. Huang Y, Isharwal S, Haese A, Chun FK, Makarov DV, Feng Z, et al. Prediction of patient-specific risk and percentile cohort risk of pathological stage outcome using continuous prostate-specific antigen

measurement, clinical stage and biopsy Gleason score. BJU Int 2011; 107:1562–9.
28. Chun FK, Karakiewicz PI, Huland H, Graefen M. Role of nomograms for prostate cancer in 2007. World J Urol 2007;25:131–42.
29. Fernandes ET, Sundaram CP, Long R, Soltani M, Ercole CJ. Biopsy Gleason score: how does it correlate with the final pathological diagnosis in prostate cancer? Br J Urol 1997;79:615–7.
30. Delso G, Furst S, Jakoby B, Ladebeck R, Ganter C, Nekolla SG, et al. Performance measurements of the Siemens mMR integrated whole-body PET/MR scanner. J Nucl Med 2011;52:1914–22.
31. Rothke MC, Afshar-Oromieh A, Schlemmer HP. Potential of PET/MRI for diagnosis of prostate cancer. Radiologe 2013;53:676–81.
32. Epstein JI. Prognostic significance of tumor volume in radical prostatectomy and needle biopsy specimens. J Urol 2011;186:790–7.
33. Breeuwsma AJ, Pruim J, Jongen MM, Suurmeijer AJ, Vaalburg W, Nijman RJ, et al. *In vivo* uptake of [11C]choline does not correlate with cell proliferation in human prostate cancer. Eur J Nucl Med 2005; 32:668–73.
34. Reske SN, Blumstein NM, Neumaier B, Gottfried HW, Finsterbusch F, Kocot D, et al. Imaging prostate cancer with 11C-choline PET/CT. J Nucl Med 2006;47:1249–54.
35. Wilt TJ, Brawer MK, Jones KM, Barry MJ, Aronson WJ, Fox S, et al. Radical prostatectomy versus observation for localized prostate cancer. N Engl J Med 2012;367:203–13.
36. Ahmed HU, Hindley RG, Dickinson L, Freeman A, Kirkham AP, Sahu M, et al. Focal therapy for localised unifocal and multifocal prostate cancer: a prospective development study. J Lancet 2012;13: 622–32.